Nanotechnology **19** (2008) 025603 (5pp) doi:10.1088/0957-4484/19/02/025603

A preliminary investigation into the new class of lithium intercalating $LiNiSiO_4$ cathode material

N Jayaprakash, N Kalaiselvi[1] and P Periasamy

Central Electrochemical Research Institute, Karaikudi, 630 006, India

E-mail: kalakanth2@yahoo.com

Received 10 July 2007, in final form 17 October 2007
Published 6 December 2007
Online at stacks.iop.org/Nano/19/025603

Abstract

A unique attempt to exploit silicate chemistry for a possible enhancement of the electrochemical properties of a lithium ion system via exploration of the novel category lithium intercalating $LiNiSiO_4$ cathode has been made through the present study. A novel citric acid assisted modified sol–gel method (CAM sol–gel) has been adopted to synthesize the title compound with a formation temperature positioned well below 500 °C, as derived from thermal studies. A powder x-ray diffraction (PXRD) pattern evidenced the absence of undesirable peaks and confirmed the formation of a hexagonal lattice structure with enhanced crystallinity and phase purity, and the presence of uniformly distributed particles of ∼200 nm size with well defined grain boundaries is obvious from the scanning electron microscopy (SEM) image of $LiNiSiO_4$ material. Further, magic angle spinning (MAS) ^7Li nuclear magnetic resonance (NMR) results from $LiNiSiO_4$ confirmed the presence of a layered type of crystal arrangement. A cyclic voltammetry (CV) study performed on a $LiNiSiO_4$ cathode revealed an excellent reversibility without any change in the peak position upon extended cycling, thus substantiating the structural stability upon progressive cycling.

(Some figures in this article are in colour only in the electronic version)

1. Introduction

The drastic technological development of today's mobile society demands a suitable energy storage device to power the multifarious requirements such as portable electronics, hybrid electric vehicles (HEV) and camcorders, cellular phones and computers (3C) applications. In this regard, lithium batteries have the highest energy density of all the commercialized rechargeable batteries, which is mainly due to the high battery voltage and large charge density of the anode active material such as lithium and carbon [1]. As a result, the lithium intercalating cathode material needs a more exploratory outlook so as to meet with the lithium chemistry requirements. The well known limitations of $LiCoO_2$ that include safety concerns have stimulated a drive to investigate certain alternative lithium-insertion electrodes that has resulted in the identification of a variety of newer cathodes for lithium batteries [2]. Hence, research on the exploitation of eco-benign and structurally stable $LiFePO_4$ phospho-olivines [3], popularly known for their low cost, nontoxicity, environmental friendliness, and high safety advantages, is gaining paramount importance. However, the low electronic conductivity [4] and slow lithium ion diffusion across the $LiFePO_4/FePO_4$ boundary [5] are critical issues against its practical application.

On the other hand, Nyten *et al* [6], followed by Dominko *et al* [7], have recently succeeded in exploiting certain silicates, namely Li_2FeSiO_4 and Li_2MnSiO_4, as lithium battery cathode materials with a reversible capacity of about 84% (∼140 mA h g^{-1}) of the theoretical capacity. Having been intrigued by such an explorative preliminary study on silicate cathodes, it was aimed through the present study to introduce Ni in the place of Fe to form a $LiSiNiO_4$ cathode for lithium battery applications. Herein, it is expected that the polyhedra of SiO_4^{4-} will make a loose structure to form an ion channel for lithium-ion conduction whereas the counter cation [8], say Ni in the present case, may stabilize the lithium ion channel. In addition, it is reported by Nakayama *et al* [9] and Sato *et al* [10, 11] that the conductivity of the lithium silicate compounds has a major dependence on the type of crystal lattice of the

[1] Author to whom any correspondence should be addressed.

cathode material. In other words, compounds belonging to hexagonal systems are reported to exhibit higher conductivity than orthorhombic ones. Hence, the hexagonal $LiNiSiO_4$ is expected to encompass an enhanced conductivity behavior along with the requisite electrochemical characteristics of lithium-ion chemistry.

Based on this ground, a first-ever attempt has been made to synthesize a novel and highly conductive $LiNiSiO_4$ compound, with a hexagonal lattice structure. It is further believed that the proposed $LiNiSiO_4$ cathode would alleviate problems such as irreversible capacity loss and poor electronic conductivity that are associated respectively with the popular candidates, namely $LiCoO_2$ and $LiFePO_4$, which is the significance of the present study.

As understood from our earlier investigations [12], the CAM sol–gel (citric acid assisted modified sol–gel) method has been adopted to synthesize the title compound, which was characterized subsequently for physical as well as electrochemical properties.

2. Experimental details

2.1. Synthesis procedure

The $LiNiSiO_4$ active material was synthesized by adopting the citric acid assisted modified sol–gel (CAM sol–gel) method, wherein the reaction proceeds in an acidic environment created by the addition of an organic acid. Stoichiometric proportions of high purity respective metal acetates, namely, CH_3COOLi, $(CH_3COO)_2Ni$ and SiO_2 (Sigma Aldrich, India) were dissolved in triple-distilled water. The contents in the beaker were allowed to react until fumes appeared, and a calculated quantity of citric acid was added as a complexing agent, followed by the addition of acrylamide and $N'N$-methylene bis acrylamide. Here, both the acrylamide and $N'N$-methylene bis acrylamide act as gelling agents, whereas citric acid, with a molecular formula of $C_6H_8O_7{\cdot}H_2O$, catalyses the bond formation between metal ions and silicon. Originally the carboxylic acid group that is present in the complexing agent forms a chemical bond with the metal ions, which upon evaporation of solvent leads to the formation of a viscous resin-like precursor. Herein, it is presumed that the metal ions are trapped inside the so-called viscous resin-like paste to ensure a atomic level mixing, which is the key point of the CAM sol–gel method.

The viscous resin-like paste thus obtained was heat treated initially at 120 °C for 12 h, followed by sintering at 300 °C for about 5 h to expel the trace amount of water and carbon in the form of CO_2. Subsequently, the sintered precursor was ground to yield finer powder and heat treated further at a higher temperature of 750 °C using an alumina crucible. Herein, both the rate of heating and cooling were maintained at 1°C min^{-1} to avoid surface cracking of the particles and to ensure the presence of uniformly distributed particles of sub-micron size. Also, it is noteworthy that the properly controlled and duly monitored heating sequence of the current study renders an improved yield of the final product without any undesirable agglomeration that takes place normally during a high temperature sintering process.

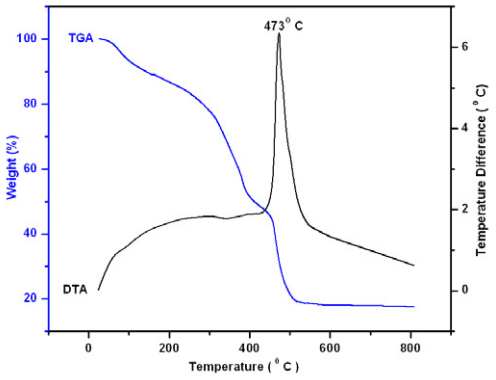

Figure 1. TG-DTA curves of $LiNiSiO_4$ precursor recorded from ambient to 800 °C with a heating rate of 10 °C min^{-1} under air.

2.2. Physical and electrochemical characterization

Thermogravimetry and differential thermal analysis (TG-DTA) curves were obtained with a thermo balance model STA 409PC in the temperature range 0–800 °C, using alumina crucibles with 25 mg of samples, under air at a heating rate of 20 °C min^{-1}. Phase characterization was done by the powder x-ray diffraction technique on a Philips 1830 x-ray diffractometer using Ni-filtered Cu Kα radiation (λ = 1.5406 Å) in the 2θ range 10°–80° at a scan rate of 0.04° s^{-1}. The surface morphology and percentage composition of the elements present in $LiNiSiO_4$ were investigated using scanning electron microscopy coupled with EDAX (energy-dispersive x-ray analysis) obtained from Jeol S-3000 H scanning electron microscope. A Fourier transform infrared spectroscopic (FTIR) study was performed on a Perkin-Elmer paragon-500 FTIR spectrophotometer using a pellet containing a mixture of KBr and the $LiNiSiO_4$ active material in the region 400–2000 cm^{-1}. NMR measurements were carried out with a Bruker MSL-400 spectrometer employing a 5 mm Bruker VT-MAS probe operating at a ^{7}Li frequency of 14 MHz. A one-pulse sequence was used, with a pulse length of 3 μs, a recycle delay of 500 ms and a minimum of 100 000 scans. Electron spin resonance (ESR) measurement was carried out using a Bruker instrument. Room temperature electrochemical studies such as cyclic voltammetry (CV) and electrochemical impedance spectroscopy (EIS) measurements were performed using an Autolab Electrochemical Workstation wherein impedance data were measured over a frequency range 100 kHz–0.1 Hz.

3. Result and discussion

3.1. Thermal analysis—TG-DTA

Figure 1 exhibits the result of simultaneous thermogravimetric-differential thermal analysis (TG-DTA) of a mixture containing the precursors of $LiNiSiO_4$, wherein the TG curve presents four steps of weight loss. The initial weight loss observed in the range of 35–180 °C is assigned to the process of dehydration that results in the complete removal of a small quantity of physically absorbed water molecules from the precursor mixture [13]. Subsequently, a substantial weight loss in the temperature range 260–350 °C is seen, and it could be ascribed to the combined decomposition of unreacted or excessive citric

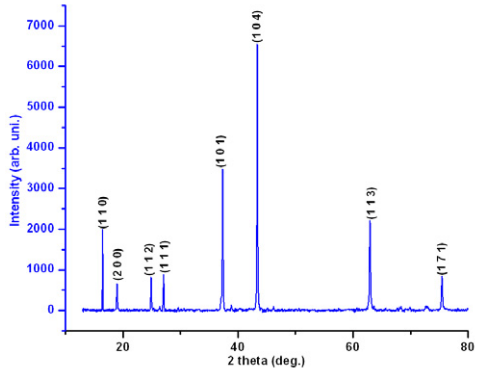

Figure 2. X-ray diffraction pattern of $LiNiSiO_4$ calcined at 750 °C.

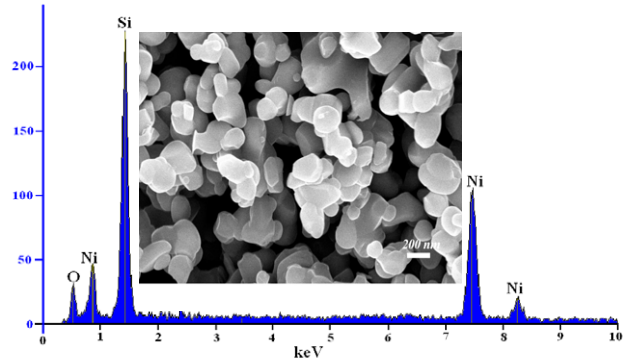

Figure 3. Scanning electron micrographs and EDAX spectra obtained from an area scan of a micrograph of $LiNiSiO_4$.

acid and acrylamide present in the precursor. Further weight loss in the temperature range 350–475 °C corresponds to the combustion of organic constituents containing complexed metal acetates and citric acid [14], which is obvious from the large exothermic peak at around 473 °C in the DTA curve. Finally, a slow and continuous decrease in weight of the precursor mix above 475 °C is seen, which may be attributed to the process of crystallization of newly formed $LiNiSiO_4$ oxide particles [15].

3.2. Structural results—PXRD studies

An x-ray diffraction (XRD) pattern of the sintered $LiNiSiO_4$ material is shown in figure 2. All the observed diffraction lines are indexed to a hexagonal crystal structure, and the absence of undesirable peaks demonstrates the presence of phase-pure product. Herein, the deployment of optimum synthesis temperature (750 °C) with an intermittent grinding has resulted in the formation of highly crystallized product, as obvious from peaks with very high intensity. The Miller indices (*hkl*) of all the peaks of $LiNiSiO_4$ powders were obtained (figure 2) and the lattice parameter values calculated from the assigned Miller indices were found to be $a = 5.18$ and $c = 11.21$. The average grain size D calculated using Scherrer's formula was found to be 140 nm, which is also comparable with the results obtained from SEM studies.

3.3. Morphological results—SEM analysis

The powder morphology of $LiNiSiO_4$ material synthesized at 750 °C is furnished in figure 3. Despite the presence of a few aggregates of small crystallites, an uniform distribution of particles is observed for the sample. Further, an approximate particle size of 200–300 nm has been exhibited by $LiNiSiO_4$ synthesized through the study, which is in accordance with the theoretical crystallite size deduced from XRD studies. Generally, sintering the precursor above 700 °C makes the particles to fuse together partially to form large porous agglomerates regardless of post-grinding treatment after the decomposition step [16]. However, neither an increased particle size nor particle agglomeration was found in the present case, which is the significance of the CAM sol–gel method. Further, the stoichiometry of the $LiNiSiO_4$ cathode has been verified using EDAX analysis (figure 3). Since it is not practically possible to calculate the percentage of lithium present in the synthesized compound by applying EDAX, the stoichiometry of Si, Ni and O were examined, wherein a unimolar ratio of Si to Ni was found, as is evident from figure 3.

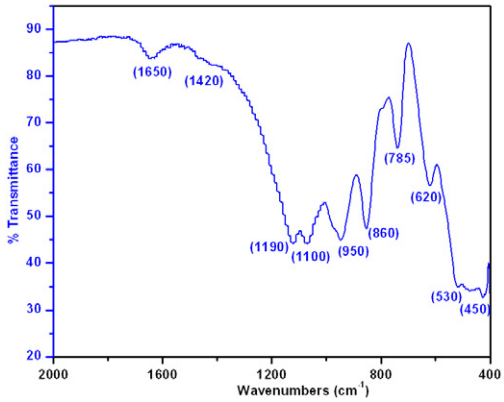

Figure 4. FTIR spectra of $LiNiSiO_4$.

3.4. Local cation environment—FTIR study

FTIR signatures of $LiNiSiO_4$ material synthesized via the CAM sol–gel method are depicted in figure 4. The vibrational frequencies at 1190, 1110 and 785 cm^{-1} are attributed to the possible stretching and bending vibrational modes of Si–O–Si and O–Si–O groups [17]. The band observed around 450 and 620 cm^{-1} may be ascribed to the asymmetric bending modes of O–M–O bonds [18]. Similarly, the FTIR signature observed near 860 cm^{-1} and a slight deviation around 1420 cm^{-1} may be corroborated to the presence of Ni–O bonds [18]. Since the FTIR signals are recorded in the range 400–2000 cm^{-1}, the resonant frequencies of alkali metal cations in their octahedral interstices (LiO_6) that are located in the frequency range of 200–400 cm^{-1} [19] become out of scope of the present study.

3.5. ^{7}Li MAS-NMR spectral studies of $LiNiSiO_4$ compound

Generally, lithium ions are either exchanged into the layers or adsorbed on the surface of the basic matrix of the ABO_4 active material upon synthesis, and the same will directly affect the electrochemical performance of the electrode. In this regard, solid-state NMR is normally used to investigate the location of lithium in the synthesized material. Figure 5 shows the broad ^{7}Li NMR spectra recorded for $LiNiSiO_4$ at room temperature.

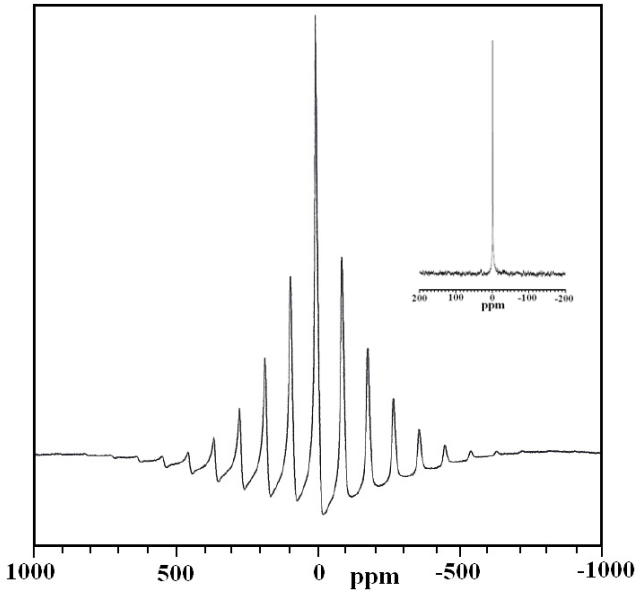

Figure 5. ^{7}Li MAS-NMR spectra of $LiNiSiO_4$ (shown in the inset is the NMR spectra of standard species CH_3COOLi).

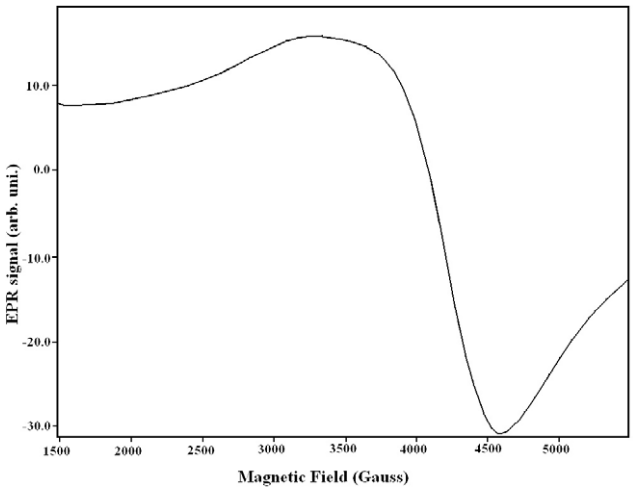

Figure 6. ESR spectra of $LiNiSiO_4$ crystalline powder.

For the ^{7}Li nucleus ($I = 3/2$) of $LiNiSiO_4$, a single central transition line at 1.47 ppm with large spinning side bands were observed, due to the quadrupole broadening of the satellite lines [20]. Further, it is understood from the study that the layered (O3) $LiNiSiO_4$ (figure 5) is diamagnetic, as the ^{7}Li NMR spectra show a resonance at 1.4 ppm that corresponds to the presence of lithium in a diamagnetic local environment. Similarly, the presence of low spin Ni ions are also evident from the NMR study (figure 5). Hence, the layered structure of $LiNiSiO_4$ compound, as deduced from the ^{7}Li MAS-NMR spectrum, stands in line with the structural elucidation results derived from the XRD pattern of $LiNiSiO_4$.

3.6. ESR spectral studies

The ESR spectra of $LiNiSiO_4$ crystalline powder are depicted in figure 6. The frequency of the microwave field is 9.778 GHz and the frequency of the ac modulation magnetic field is 100 kHz. Under such conditions, the ESR signal is centered at 3480 G (figure 6). The ESR signal of $LiNiSiO_4$ is found to be very weak, which may generally be attributed and correlated to the magnetic defects present within the compound or impurity features presumably due to the configuration of the Ni^{2+} ion as inferred from the CV studies. So in the present case, the weak signal is assigned to the presence of two unpaired or uncoupled electrons associated with the low spin Ni^{2+} configuration ($t_{2g}^6 e_g^2$: $t_{2g}[d(xy)^2 d(yz)^2 d(zx)^2] e_g[(dx^2 - y^2)^1 (dz^2)^1]$). As reported, this kind of defect is very sensitive to its local neighborhood, and may result in the large broadening of the EPR line [21], which thus results in the ESR pattern of the observed type (figure 6).

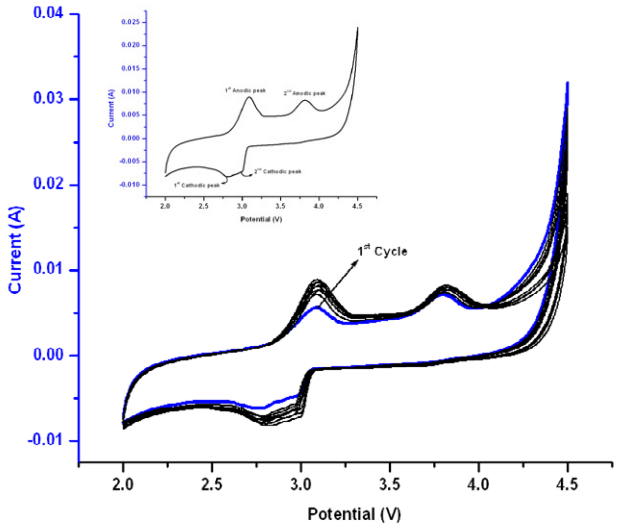

Figure 7. Representative cyclic voltammograms of $LiNiSiO_4$ at a scan rate of 1 mV s^{-1} (shown in the inset is the representative first scan).

3.7. Electrochemical properties of LiNiSiO$_4$

Prior to the recommendation of $LiNiSiO_4$ as a possible lithium intercalating cathode for potential lithium battery applications, the electrochemical properties of the same has been examined by impedance and cyclic voltammetry studies. Figure 7 shows the representative cyclic voltammogram of the $LiNiSiO_4$ compound reported at room temperature under a scan rate of 1 mV s^{-1} between a potential range of 2.0 to 4.5 V versus Li/Li^+. The CV pattern shows two anodic peaks at 2.9 and 3.9 V and a corresponding pair of cathodic peaks at 3.0 and 2.8 V. It is quite interesting to note that the peak current of the successive cycles becomes larger and narrower along with a perfect overlapping of redox peaks produced upon progressive cycles. This is an indication that the synthesized $LiNiSiO_4$ cathode exhibits excellent electrochemical reversibility, especially upon progressive cycling processes, thus qualifying the same for practical applications.

The pair of anodic and cathodic peaks observed around 2.9 and 2.7 V may be attributed to a Li^0/Li^+redox couple [21] and the second pair of anodic and cathodic peaks at 3.9 and 3.0 V is ascribed to the redox reaction of Ni^{2+}/Ni^{4+}, based on

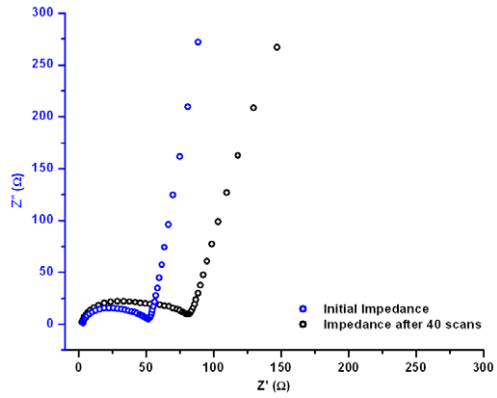

Figure 8. Nyquist impedance spectra of $LiNiSiO_4$.

the reports Lu *et al* [22] and Kang *et al* [23]. As there is no apparent change in the peak position or peak current value in the cyclic voltammogram of the $LiNiSiO_4$ cathode even after 40 scans (figure 7), the stability of cycling with no significant structural degradation during the lithium extraction/insertion process could be understood.

The high stability of the $LiNiSiO_4$ cathode upon cycling was further confirmed from the electrochemical impedance analysis. The electrochemical impedance spectroscopy was measured for both the as-fabricated cell and the cell after completing 40 cycles. Herein, 2016 coin cells containing the synthesized $LiNiSiO_4$ cathodes, lithium metal anode and an electrolyte consists of 1 M $LiPF_6$ in ethylene carbonate (EC): dimethyl carbonate (DMC) were fabricated and deployed for impedance analysis. Figure 8 shows the typical Nyquist plot recorded for the cells fabricated using the synthesized $LiNiSiO_4$ materials. The impedance plot consists of a depressed semicircle in the high and medium frequency region that results respectively from an ionically conducting and an electronically insulating electrode surface layer, and the charge-transfer process. Also, a line at low frequency is observed which is associated with solid-state diffusion of Li^+ ions into the bulk cathode material, otherwise known as Warburg diffusion [24]. In the high frequency region, the intercept values with the real impedance [Re(Z)] are 60 and 80 Ω respectively, corresponding to the as-fabricated $LiNiSiO_4$ cell and the cell after 40 cycles. It is well known that such an intercept value is considered as the total electrical resistance offered by the electrode material (R_m), electrolyte (R_e), and the electrical leads (R_l) [25] Since the R_e and R_l values are almost the same throughout the experiments the small difference in the total resistance value observed for the $LiNiSiO_4$ cathode corresponds to the low resistance offered by the same upon extended cycling.

4. Conclusion

A novel $LiNiSiO_4$ lithium intercalating cathode material has been synthesized by adopting the CAM sol–gel method. The chosen method is found to be advantageous in producing a nanocrystalline $LiNiSiO_4$ product with preferred physical and electrochemical properties that are required for rechargeable lithium battery applications. The XRD and ^7Li NMR studies support the formation of $LiNiSiO_4$ with a hexagonal crystal lattice structure, and the finer particles are found to be ∼200 nm in size. The weak signal of the ESR spectrum and the presence of redox peaks around 3.9 and 3.0 V in CV studies support the presence of low spin Ni^{2+} ions. The excellent cyclic reversibility and enhanced conductivity of the compound as identified from CV studies and impedance analysis authenticate the possibility of exploiting the synthesized $LiNiSiO_4$ material as a novel cathode suitable for new generation lithium ion battery application.

Acknowledgments

The authors are thankful to the Department of Science and Technology (DST), New Delhi, for financial support to carry out this work. Also, the authors thank Dr S Radhakrishnan for recording ^7Li NMR.

References

[1] Wang J, Yang J, Wan C, Du K, Xie J and Xu N 2003 *Adv. Funct. Mater.* **13** 487
[2] Chebiam R V, Kannan A M, Prado F and Manthiram A 2001 *Electrochem. Commun.* **3** 624
[3] Li G, Azuma H and Tohda M 2002 *Electrochem. Solid-State Lett.* **5** A135
[4] Wang Y, Wang J, Yang J and Nuli Y 2006 *Adv. Funct. Mater.* **16** 2135
[5] Padhi K, Nanjundaswamy K S and Goodenough J B 1997 *J. Electrochem. Soc.* **144** 188
[6] Nyten A, Abouimrane A, Armand M, Gustafsson T and Thomas J O 2005 *Electrochem. Commun.* **7** 156
[7] Dominko R, Bele M, Gaberscek M, Meden A, Remskar M and Jamnik J 2006 *Electrochem. Commun.* **8** 217
[8] Matsumoto H, Yonezawa K and Iwahara H 1998 *Solid State Ion.* **113–115** 79
[9] Nakayama S and Sakamoto M 1992 *J. Ceram. Soc. Japan* **100** 867
[10] Sato M, Kono Y, Ueda H, Uematsu K and Toda K 1996 *Solid State Ion.* **83** 249
[11] Sato M, Kono Y and Uematsu K 1994 *Chem. Lett.* **23** 1425
[12] Jayaprakash N, Sathiyanarayanan K and Kalaiselvi N 2007 *Electrochim. Acta* **52** 2453
[13] Hermanek M, Zboril R, Mashlan M, Machala L and Schneeweiss O 2006 *J. Mater. Chem.* **16** 1273
[14] Yoon W S and Kim K B 1999 *J. Power Sources* **81/82** 517
[15] Jayaprakash N, Kalaiselvi N and Periasamy P 2007 *Electroanal. Chem.* submitted
[16] Hu Y, Doeff M M, Kostecki R and Finones R 2004 *J. Electrochem. Soc.* **51** A1279
[17] Liang Y, Fan J, Xia X H, Luo Y S and Jia Z J 2007 *Electrochim. Acta* **52** 5891
[18] Kalyani P and Kalaiselvi N 2005 *Sci. Technol. Adv. Mater.* **6** 689
[19] Jayaprakash N and Kalaiselvi N 2007 *Electrochem. Commun.* **9** 620
[20] Nakamura K, Nishioka D, Michihiro Y, Vijayakumar M, Selvasekarapandian S and Kanashiro T 2006 *Solid State Ion.* **77** 129
[21] Zaghib K, Salah A A, Ravet N, Mauger A, Gendron F and Julian C M 2006 *J. Power Source* **160** 1381
[22] Lu Z H, Beaulileu L Y, Donaberger R A, Thomas C L and Dahn J R 2002 *J. Electrochem. Soc.* **149** A778
[23] Kang S H, Kim J, Stoll M E, Abraham D, Sun Y K and Amine K 2002 *J. Power Sources* **112** 41
[24] Lee C Y, Tsai H M, Chuang H J, Li S Y, Lin P and Tseng T Y 2005 *J. Electrochem. Soc.* **152** A716
[25] Zhou Y K, He B L, Zhou W J and Li H L 2004 *J. Electrochem. Soc.* **151** A1052